arXiv:1402.2517v2 [cond-mat.mtrl-sci] 17 Jul 2014

Taming the resistive switching in Fe/MgO/V/Fe magnetic tunnel junctions: An ab initio study

J.M. Aguiar-Hualde
IPhT, CEA/Saclay, Orme des Merisiers, 91190 Gif-sur-Yvette Cedex, France.

M. Alouani
IPCMS, UMR 7504 CNRS-UdS, 23 rue du Loess, Strasbourg 67034, France.

A possible mechanism for the resistive switching observed experimentally in Fe/MgO/V/Fe junctions is presented. Ab initio total energy calculations within the local density approximation and pseudopotential theory shows that by moving the oxygen ions across the MgO/V interface one obtains a metastable state. It is argued that this state can be reached by applying an electric field across the interface. In addition, the ground state and the metastable state show different electric conductances. The latter results are discussed in terms of the changes of the density of states at the Fermi level and the charge transfer at the interface due to the oxygen ion motion.

INTRODUCTION

Bipolar nonvolatile Resistive Switching (RSw), is one of the most largely studied phenomena [1–4] for the development of next generation of random access memory (RAM) devices. Some of these devices have a metal-insulator-metal (M/I/M) structure like graphene oxides (GO) of the form Cu/GO/Pt. In these systems, the RSw was explained [5] in terms of desorption/absorption of oxygen-related groups on the GO sheets and the diffusion on the top Cu electrodes. MgO-based magnetic-tunnel junctions (MTJ) are also good candidates for RAM memories since it was shown that they have good RSw reproducibility [6]. One of the aspects that makes them particular, is that they can exhibit two kinds [7] of switching: magnetoresistive and structural (RSw). This enlarge the scope of applicability of these memories.

Despite the great interest on the tunneling magnetoresistance (TMR) features of these kind of junctions due to the large values predicted by Butler and coworkers for Fe/MgO/Fe [8], the mechanism for the RSw phenomenon remains to be elucidated. However, in the last few years, several possible mechanisms have been proposed [9]. For example, to explain the bipolar RSw, three different effects are mentioned in the literature. The first one is the electrostatic/electronic effects, the second the electrochemical metalization (ECM) effect, and the third the valence change memory (VCM) effect. The first effect is based on purely electronic phenomena, like those induced by charge traps [10, 11]. The other two effects involve oxidation-reduction (redox) processes. In ECM, ions travel across the insulating spacer from the active electrode to the inert electrode, developing dendrites, while in VCM, the migration of anions takes place when applying a voltage pulse and produces reduction or oxidation reactions depending on the polarity [3, 4]. According to the theory of filamentary conduction [12], the redox reactions take place across the filaments grown along defects in the insulating spacer. The size of the MgO spacer seems also to play an important role [7], e.g., thin MTJs usually exhibit RSw from the virgin state, while thick ones go through an electroforming process (in which filaments are developed) before displaying the phenomenon. Some models [13] have been proposed to simulate the filamentary conduction on transition-metal oxides.

The models that describe the RSw, rely usually on an assumption of two local minima in the energy profile. Recently, a double well model for trapped electrons in MgO-based tunnel junctions [14] confirm the power law dependencies of resistance observed experimentally [15].

Using first principle transport calculation[16, 17], it is shown that the tunneling magnetoresistance "TMR" of Fe/MgO/Fe junctions is strongly diminished by small oxygen concentrations in a single partially oxidized FeO interface layer. This reduction is attributed to the reduction of specular contributions to the conductances of the parallel configuration of the lead magnetizations highlighting the importance of ordered interfaces for large TMR ratios. This later conclusion is also in agreement with that of Wortamnn *et al.*[18] regarding the interplay between electronic structure, atomic structure and the tunneling process. The barrier thickness in the limit of coherent tunneling is also shown to be important[19] since it is shown that at large barrier thicknesses, only a small amount of states contributes to the overall current. Another important issue concerns the interchannel diffusive scattering by disordered oxygen vacancies located at or near the Fe/MgO interface which is shown to drastically reduce the tunnel the TMR from the ideal theoretical limit to the presently observed much smaller experimental range.[20]

In the Fe/MgO/Fe junctions, the effect of the inclusion of different transition metal atomic species at one of the Fe/MgO interface has been studied. For example, chromium or vanadium were inserted as an electron symmetry filter in the system, [6, 15]. Both chromium and vanadium can be easily polarized by proximity with a magnetic material such as iron. The mem-

ristor model [21] was shown to be good for explaining the hysteresis-like I-V characteristics. The conductance of Fe/MgO/V/Fe was shown to oscillate with increasing the number of vanadium layers [22]. Another reason for including vanadium at the Fe/MgO interface, lies in the higher oxygen affinity of this element compared to iron. This would make it possible for the appearance of oxygen vacancies at the interface and would break the symmetry of the sample defining the active electrode. This is one of the aspects which lead to the bipolar behavior of the switching.

Usually, V is assumed to lie on top of O when grown on MgO substrate, however this was shown not to be always the case by Ikuhara and coworkers [23]. In a study of the atomic and electronic structure of V/MgO interface, they showed that the best matching between experiment and simulation corresponds to the case when V is located on top of Mg. This geometry allows the oxygen ions to move in straight line across the interface when redox reactions take place.

In this work, we focus on the study of the RSw on Fe/MgO/V/Fe with the goal of gaining insight into the mechanism of this interesting phenomenon. To this end, we performed our study by computing the total energy of the system for various motions of the oxygen ions at the MgO/V interface and restrict ourselves to the case of ferromagnetic alignment of the iron electrodes. The main goal pursued in this work is to show whether it is possible to find two local minima in the total energy profile by identifying two possible positions for an oxygen ion moving across the MgO/V interface. This will simulate the oxidation which is assumed to take place in the RSw phenomenon as suggested by experiment in the case of $KNbO_3$[3].

The geometrical configuration of the system with the oxygen ion in the MgO layer, is referred to as the initial state configuration, while the final configuration corresponds to the oxygen in the position identified by the minimum of the total energy. To achieve this goal, we tried several types of atomic arrangements in order to contrast the results and optimize the way to simulate the oxidation. The zero bias electrical conductance is then computed and the results are discussed in reference to those obtained experimentally. Notice however that the experimental thickness of the MgO insulating barrier of about 3 nm is much larger that the one used in our calculation which is less than one nm. Due to this sever limitation, our calculations can only be compared qualitatively to the experimental results.

COMPUTATIONAL DETAILS

The electronic conductance was calculated using the SMEAGOL [24] package where the non-equilibrium Green's function formalism is employed. In this code, the ballistic regime is assumed so the Landauer-Büttiker formula for the current is valid for computing the electric current. To compute the conductance, we have used 400×400 **k** points in the two dimensional Brillouin zone as used in Ref. [22]. This high mesh is required for the good convergence of the conductance. The electronic structure required for the calculations, is performed by means of the SIESTA code [25] which is a density functional theory (DFT) code based on the pseudopotential approximation and localized numerical orbital basis set. Apart from specifying the structural parameters of our system, we have to chose the type of exchange-correlation (XC) functional, the pseudopotentials (PPs) for the atomic species, and the size of the basis set. For this study, the PPs were generated using the improved Troullier-Martins scheme[26]. The local density approximation (LDA) was employed for both the generation of the pseudopotentials and the exchange-correlation potential [27]. Non-linear exchange-correlation core corrections were used for iron, vanadium and magnesium and no core corrections for oxygen. The electronic population and the cutoff radii for each atomic species and angular momentum are listed in Table I.

Orbital	Fe	V	Mg	O
s	$4s^2$ 2.00	$4s^2$ 2.97	$3s^2$ 2.50	$2s^2$ 1.25
p	$4p^0$ 2.24	$4p^0$ 3.50	$3p^0$ 2.50	$2p^4$ 1.25
d	$3d^6$ 1.78	$3d^3$ 1.59	$3d^0$ 2.50	$3d^0$ 1.25
f	$4f^0$ 2.00	$4f^0$ 2.17	$4f^0$ 2.50	$4f^0$ 1.25

TABLE I: Electronic configuration (left) and cutoff radii for each atomic species and angular momentum.

For the basis set, a split-valence type was used with a split norm value of 0.15. Double-ζ type was employed for all the atoms and angular momentum while polarization functions was used only for iron, vanadium and magnesium. The values chosen for the cutoff radii of the first ζ are summarized in Table II. The values for the cutoff radii of the second ζ were left to be determined by the split norm value. The electronic temperature and the mesh cutoff are set to 300K and 350 Ry, respectively. The structural parameters were those of Butler and coworkers [8]: iron sits on top of oxygen with a distance of 2.16 Å, vanadium occupies the place of iron in the interface V/MgO. The iron lattice constant is 2.866 Å and MgO lattice constant is $\sqrt{2}$ times that of the Fe. As mentioned before, following the work of Ikuhara and coworkers on V/MgO interfaces [23] we have also studied the positioning of V on top of Mg.

Fe	V	Mg	O
$4s$: $r_c = 6.0$	$4s$: $r_c = 6.0$	$3s$: $r_c = 6.0$	$2s$: $r_c = 4.0$
$3d$: $r_c = 5.0$	$3d$: $r_c = 5.0$		$2p$: $r_c = 4.5$

TABLE II: Cutoff radii for the first ζ basis function for each atom and angular momentum.

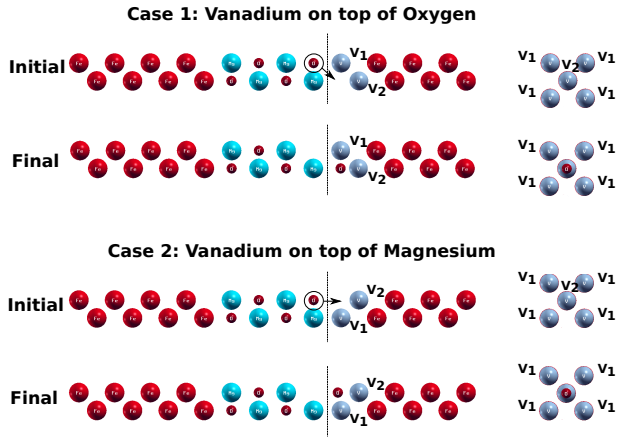

FIG. 1: Initial and final unit cells for the two cases considered: the vanadium is on top of oxygen (top drawings) and V on top of Mg (bottom drawings). The motion of oxygen ion is shown by an arrow. The first and second layer of vanadium (V_1 and V_2) are identified for further reference. For clarity, the interface at the vanadium 1 is shown on the right in xy plane for the initial and final states.

RESULTS AND DISCUSSION

Total energy local minimum due to oxygen motion

The motion of oxygen ions may take place when defects or oxygen vacancies are present [3]. This could be the reason for the none existence of resistive switching in Fe/MgO/Fe systems: introducing vanadium in one of the Fe/MgO interfaces, defects and dislocations are more likely to appear, and in this way, negatively charged oxygen ions have more space where to migrate under an applied electric field.

Fig. 1 depicts the initials and final configurations on the 2 cases considered in this work: vanadium on top of oxygen and vanadium on top of magnesium. Fig. 2 shows the results for the average total energy per atom as a function of the oxygen position (only the $\hat{z}$ component, orthogonal to the interface planes) for all the cases considered. In order to compare the results, all the curves are relatives to the energy of the initial configuration, i.e. when the oxygen ion is in its initial state. Curve (a) corresponds to the case taken as a reference for the other possible paths. In this case, we considered a relatively small unit cell (24 atoms) and the oxygen ion in front of

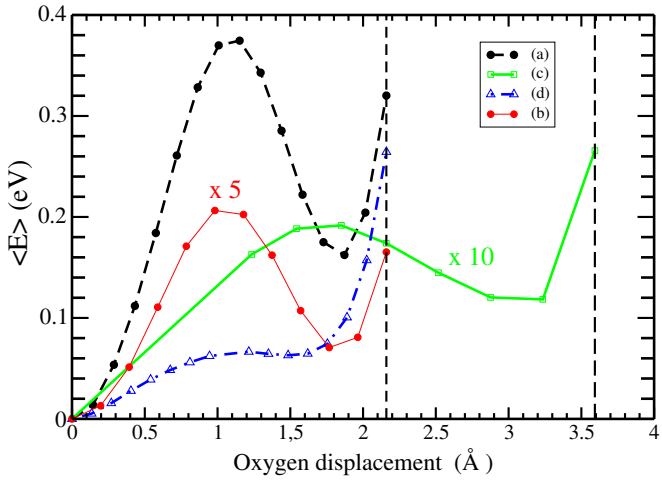

FIG. 2: Average total Energy per atom in eV as a function of oxygen displacement in (Å) for the several cases of oxygen motion : (a) small unit cell; (b) large unit cell and only one oxygen is allowed to move; (c) large unit cell, V vacancy; (d) small unit cell, V on top of Mg. Cases (b) and (c) are amplified 5 and 10 times respectively. All the cases are performed within the LDA approximation. The origin of the displacement corresponds to the position of the last MgO layer, the dashed line at 2.16 Å refers to the first vanadium layer and the dashed line at 3.593 Å to the second one.

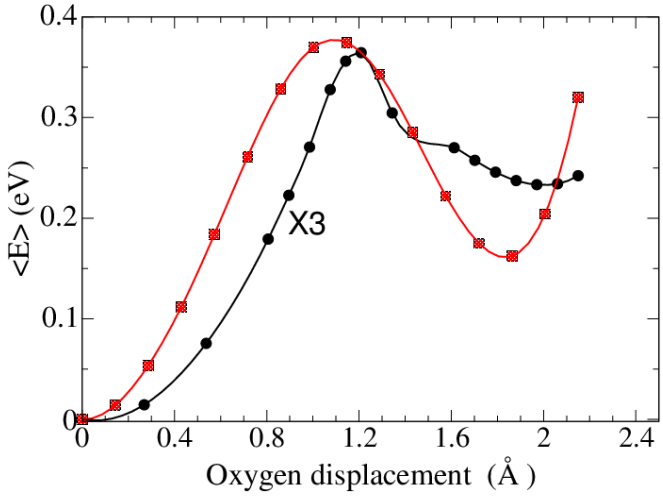

FIG. 3: Calculated average total Energy per atom in eV as a function of oxygen displacement in (Å) with total atomic relaxation (black dots) compared to the unrelaxed structure (red dots). Notice that the atomic relaxation reduces drastically the energy barrier height.

the vanadium layer is moved to oxidize that layer. It is worth noticing that the motion of the oxygen ion, is not along $\hat{z}$ direction but diagonal when there is a vanadium atom in front as is shown in figure 1. Here we observed one of the main results of this work: somewhere near 1.85 Å from the initial position, the total energy exhibits

a minimum. It can be argued that the barrier energy is very high of about 0.37 eV but this is a consequence of this kind of motion, where one oxygen ion is moved in this small unit cell. This will correspond to moving the whole oxygen layer in the last MgO layer to simulate the oxidation of vanadium. In order to validate this hypothesis, we calculated the same kind of motion but in a larger unit cell (215 atoms in total) by moving one out of 9 oxygen ions. The result presented by curve (b) shows that the barrier's height diminishes by an order of magnitude to 41 meV or when converted to temperature is about 476 K. This is a realistic barrier that can be overcome easily by an electric field. We will now explore other possible oxygen motions to reduce further the barrier height.

In Fig. 2 (c), we have considered the same large unit cell as in (b) but a vanadium vacancy in front of the oxygen. Finally, in Fig. 2 (d) we have used the same small unit cell as in (a) but V on top of Mg (case 2 in Fig. 1). In these two cases, the oxygen moves in a straight line and the last case corresponds to the geometry which Ikuhara et coworkers [23] consider more likely for a MgO/V interface. It is worth noticing that in both cases the energy barriers height diminish drastically being (c) the lowest, closer to realistic values (0.017 eV or about 197 K). Vanadium vacancies make the minimum to shift deeper into the vanadium layers while considering V on top of Mg (as suggested by Ikuhara and coworkers [23]) lowers the potential barrier. However, the second minimum at 1.5Å, is very shallow and is about 4 meV lower that the barrier height of 66.5 meV (see 2d). This shallow minimum of about 46 K can trap an oxygen ion only at low temperatures. The comparison of all these total energy calculations as a function of the position of one of the oxygen ions suggests that case (a) and (d) are the most representative of oxygen ion migration across the interface. Despite the different ways that the oxygen ion might migrate across the interface or how its motion is computed, a general feature emerges. There is a local energy minimum when an oxygen ion is moved across the interface. We argue that because the oxygen ion is electrically charged, such a motion can be triggered by an applied strong electric field pulse. The trapped negatively charge oxygen ion in this minimum can reverse motion when the electric field is applied in the opposite direction.

There are two major factors that might reduce drastically the calculated energy barrier heights. The first one is the atomic relaxations around the displaced oxygen ion which are not taken into account due to high computational cost. Nevertheless, we have performed atomic relaxation for the small unit cell in absence of an applied electric field, which is not so computationally difficult to implement. We compare in Fig. 3 the average total energy per atom as a function of the oxygen displacement for the relaxed and the not relaxed calculations. We can see that the atomic relaxations reduce drastically the energy barrier by enhancing the electronic screening around the displaced oxygen ion. However, we believe that such huge relaxation are overestimated because in presence of an applied electric field, the atoms around the displaced oxygen atoms will have less time to relax. We expect therefore that the atomic relaxations will not play a very important role. The Second factor that might reduce the barrier height involves oxygen vacancies. Experiment shows that positively charged oxygen vacancies are also important for the oxygen ions diffusion under an applied electric field [3, 4]. One therefore expects that an oxygen vacancy distribution would significantly reduce the energy barrier since the negatively charged oxygen ions will have enough space to move. Such calculations are computationally expensive and are therefore beyond the scope of the present study. Since the non optimized oxygen motion produces large energy barrier heights, it is difficult to estimate a realistic electric field that will move the oxygen ions (O2-). If we consider that $\Delta V = dE$ (where ΔV is the potential corresponding to the energy barrier, E the applied electric field, and d the displacement of oxygen ion) then for ΔV of 1 volts and d of the order of 1 Å , we need a field of at least 10^8 V/m. This is a large electric field and defect pathways and other relaxation effects are therefore necessary for reducing the energy barrier height. Notice however that experimentally the applied voltage is about 1 volt and since the potential drop will occur only through the insulating region of the order of 1 nm (see Ref. [14]), the produced electric field in MgO is of the order of 10^9 V/m which of about the same order of magnitude than the estimated electric field.

Transmission and Conductance

In Fig. 4 we present the results for the transmission as a function of energy at the initial and final configurations of the oxygen motion in both studied junctions, i.e., V on top of O (left column) and V on top of Mg (right column). Top row corresponds to the total transmission while the spin decomposition is shown in the other two columns: spin majority ($G_\uparrow$) in the center and spin minority ($G_\downarrow$) in the bottom. Comparing the rows, we notice that the total transmission has almost the same shape of the $G_\uparrow$ component. This is a consequence that in ours calculations we are considering the ferromagnetic alignment for studying the RSw of the junction. If we observe the total conductance (transmission at the Fermi level) we find that it increases when the system goes from the initial state to the final one in the case of V on top of O, but it has the opposite behavior in the case of vanadium on top of magnesium. This resistance change would be a good test for distinguishing experimentally between the two geometries, i.e., correlating the sense of the switching and the orientation of the sample with respect to the

applied electric field.

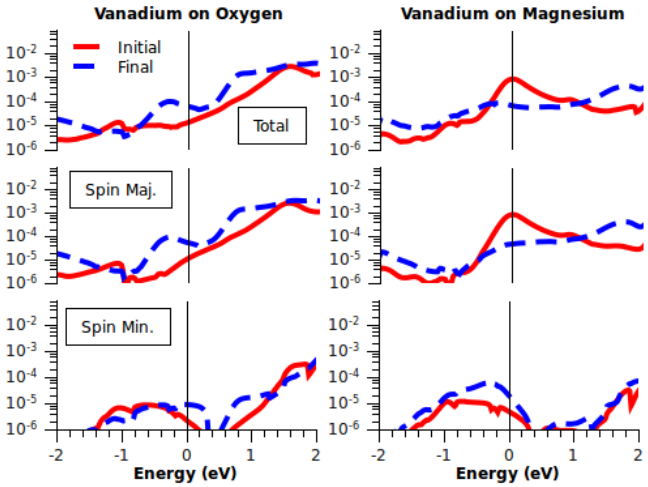

FIG. 4: Transmission as a function of energy for the initial (solid red curves) and final (dashed green curves) configurations. Left column: V on top of O; right column: V on top of Mg. Top row shows total transmissions; central row the spin majority components; and the bottom row the spin minority components. In all cases, the conductance shows a switching.

The total conductance and their spin dependent values, are summarized in table III. The labels correspond to each case in Fig. 2. Apart from case (c), where the total conductance has the same order of magnitude in both initial and final states, the total conductance of the system is one order of magnitude lower in the initial configuration than in the final one when V is on top of O, while for V on top of Mg the values are reversed. We notice also that the main spin component of the conductance is reversed when comparing vanadium on oxygen and vanadium on magnesium.

Case	$G_\uparrow/G_0$	$G_\downarrow/G_0$	G_{Total}/G_0
(a) Initial	5.83e-05	3.02e-04	3.60e-04
(a) Final	9.48e-04	1.98e-04	1.15e-03
(b) Initial	1.18e-03	4.84e-06	1.19e-03
(b) Final	3.51e-02	7.98e-06	3.51e-02
(c) Initial	4.59e-03	3.28e-06	4.59e-03
(c) Final	2.84e-03	5.13e-06	2.85e-03
(d) Initial	1.45e-02	4.52e-05	1.45e-02
(d) Final	5.90e-04	1.24e-03	1.83e-03

TABLE III: Conductance values in the initial and final configurations for all the LDA calculations in the ferromagnetic alignment. Labels correspond to those of Fig. 2

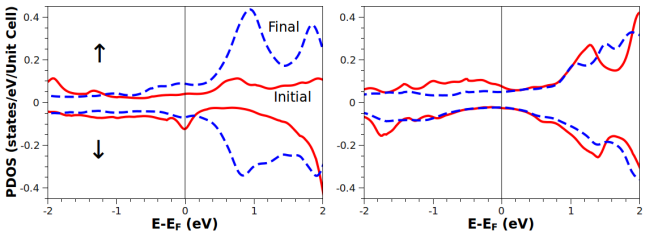

FIG. 5: $d_{3z^2-r^2}$ component of the PDOS for the vanadium atom in front of the moving oxygen (figure 1): V_1 for V on top of O (left panel) and V_2 for V on top of Mg (right panel). The Fermi level is at the zero of energy.

Density of states

From the analysis of the local density of states (PDOS) of the MgO, the highest occupied states are at about -4 eV below the Fermi level and the lowest unoccupied states are at about 2 eV above it. That gives an MgO band gap of about 6 eV. This value is much smaller than the bulk value of 7.8 eV but it seems that thin films have much smaller band gaps [28]. When the RSw takes place, the changes in the partial density of states (PDOS) occurs mainly for atoms located at the vicinity of the displaced oxygen ion. The most appreciable change, corresponds to the $d_{3z^2-r^2}$ orbital of the vanadium in front of the oxygen in the initial position: referred to as V_1 for V on top of O and V_2 for V on top of Mg (see figure 1). The results for such PDOS are shown in Fig. 5 and explain the behavior of the conductance discussed previously. The spin majority component of the PDOS around the Fermi energy (taken as the energy zero), is relevant here due to the ferromagnetic alignment of the leads. It increases in V on top of O when the oxygen moves from the initial to final position but decreases in the same situation for V on top of Mg. We can interpret this result in terms of the magnetic moment and charge transfer at the MgO/V/Fe interfaces as we will see.

Magnetic moment and charge transfer

Fig. 6 shows the charge transfer and the spin magnetic moments at the Fe/MgO/V/Fe interfaces. It is clear that at the Fe/MgO interface there is a net charge transfer from the last Fe layer towards the first MgO layer (panels (a) and (b)), and the interface iron magnetic moment is about 3 μ_B much larger than the bulk moment of 2.2 μ_B (panels (c) and (d)). This moment is typical of an iron surface and is due to a lower iron coordination. However, the MgO/V/Fe interface is much more interesting. First, when the V atom is on top of O, it is much oxidized, i.e. there is a net charge transfer from the vanadium layers towards both MgO and Fe (initial case in panel

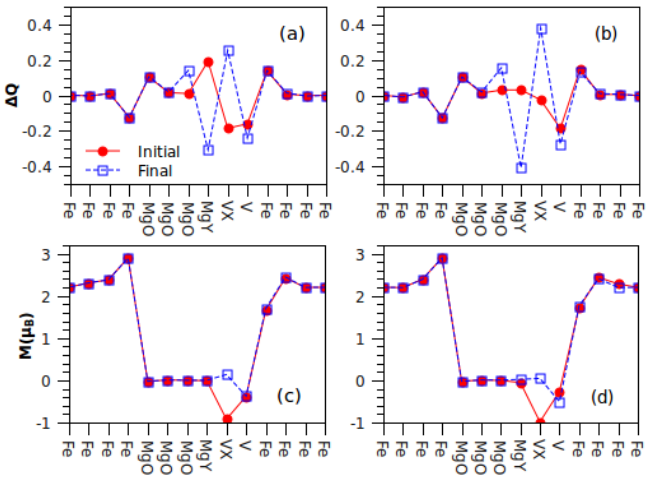

FIG. 6: Magnetic moment **M** and charge transfer ΔQ across the system; The left (a) and (c) panels are for V on top of O and the right (b) and (d) panels are for V on top of Mg. A positive ΔQ corresponds to a charge accumulation on the layer and negative one to a charge depletion. In the initial configuration X is an empty site and Y is an oxygen ion, while in the final configurations it is the other way around.

(a)). But, when one oxygen ion passes into the first V plan (final case in panel (a)), the first V layer adjacent to Mg gains about 0.25 electrons and the Mg0 layer loses about -0.3 electrons. This is essentially due to the extra charge of the displaced oxygen ion. When V is on top of Mg (panel (b)), the situation is a bit more complex in the final state. Due to the extra charge of the oxygen ion, the interface vanadium layer gains about 0.4 electron while the adjacent MgO layer loses about the same amount of charge and the second MgO layer gains about 0.15 electron. The oxygen in the vanadium layer plays the role of an impurity and creates a Friedel charge oscillation around it.

The opposite behavior observed in the conductance for both configurations in Table III, can be understood by analyzing the charge transfer presented in Fig. 6: for V on Mg (panel (a)) we have less charge oscillation in the initial configuration than the final configuration. This qualitatively favors a higher conductance for the initial configuration as shown in Fig. 4. For V on top of O, the situation is different since the charge oscillation is about the same for the initial and final configuration. However, we notice that both in the initial configuration both vanadium layers have a charge depletion which amount to higher potential barrier than in the final configuration. This might qualitatively favor a higher conductance for the final conductance and can be the origin of the opposite switching in the conductance mentioned in Fig. 4.

CONCLUSION

In this study we determined some possible paths of oxygen ions migration across the MgO/V interface of the Fe/MgO/V/Fe junction. In particular, we have shown that there is a local minimum of the total energy of the system as a function of the oxygen position at the interface. This gives an interesting scenario about how oxygen ions get trapped in a local minimum upon the application of a strong electric field pulse and how the motion of oxygen get reversed when the field is applied in the opposite direction and its connection to RSw. Moreover, it is shown that switching is different depending on how the vanadium layer is placed on top of the MgO layer (V on top of O or on top of Mg). This would establish an easy experimental way of determining the structure of the junction. In any case, the migration of the oxygen makes the RSw in MgO-based MTJ more plausible. We hope that the mechanism presented in this work clarifies somehow the RSw in MgO-based MTJ, and complements other model studies and will be useful for the elaboration of new models based on realistic calculations.

We acknowledge support from an ANR pnano grant No. ANR-06-NANO-053-01. This work was performed using HPC resources from GENSI-CINES Grant gem1100. We acknowledge helpful discussions with I. Rungger and S. Sanvito.

[1] A. Sawa, *Mater. Today* **11**, 28 (2008).
[2] R. Waser and M. Aono, *Nature Mater.* **6**, 833 (2007).
[3] K. Szot, W. Speier and W. Eberhardt *Appl. Phys. Lett.* **60**, 1190 (1992).
[4] J. J. Yang, M. D. Pickett, X. Li, D. A. A. Ohlberg, D. R. Stewart and R. S. Williams, *Nature Nanot.* **3**, 429 (2008).
[5] C. L. He, F. Zhuge, X. F. Zhou, M. Li, G. C. Zhou, Y. W. Liu, J. Z. Wang, B. Chen, W. J. Su, Z. P. Liu, Y. H. Wu, P. Cui and R.-W. Li, *Appl. Phys. Lett.* **95**, 232101 (2009).
[6] D. Halley, H. Majjad, M. Bowen, N. Najjari, Y. Henry, C. Ulhaq-Bouillet, W. Weber, G. Bertoni, J. Verbeeck and G. Van Tendeloo, *Appl. Phys. Lett.* **92**, 212115 (2008).
[7] J. M. Teixeira, J. Ventura, R. Fermento, J. P. Araujo, J. B. Sousa, P. Wisniowski and P. P. Freitas, *J. Phys. D: Appl. Phys.* **42**, 105407 (2009).
[8] W. H. Butler, X.-G. Zhang, T. C. Schulthess and J. M. MacLaren, *Phys. Rev. B* **63**, 054416 (2001).
[9] R. Waser, R. Dittmann, G. Staikov and K. Szot, *Adv. Mater.* **21**, 2632 (2009).
[10] J. G. Simmons and R. R. Verderber, *Proc. R. Soc. Lond. A* **301**, 77 (1967).
[11] M. J. Rozenberg, I. H. Inoue and M. J. Sanchez, *Phys. Rev. Lett.* **92**, 178302 (2004).
[12] G. Dearnaley, A. M. Stoneham and D. V. Morgan, *Rep. Prog. Phys.* **33**, 1129 (1970).
[13] M. J. Rozenberg, M. J. Sanchez, R. Weht, C. Acha, F. Gomez-Marlasca and P. Levy,*Phys. Rev. B* **81**, 115101

(2010).
[14] E. Bertin, D. Halley, Y. Henry, N. Najjari, H. Majjad, M. Bowen, V. DaCosta, J. Arabski and B. Doudin, *J. Appl. Phys.* **109**, 083712 (2011).
[15] N. Najjari, D. Halley, M. Bowen, H. Majjad, Y. Henry, and B. Doudin, *Phys. Rev. B* **81**, 174425 (2010).
[16] P. Bose,. A. Ernst, I. Mertig, and J. Henk, *Phys. Rev. B* **78**, 092403 (2008).
[17] C. Heiliger , P. Zahn, I. Mertig, *J. Magn. Magn. Mater.* **316**, 478 (2007).
[18] D. Wortmann, G. Bihlmayer and S. Blugel, *J. Phys.: Condens. Matter* **16**, S5819 (2004).
[19] C. Heiliger, P. Zahn, B. Yu. Yavorsky, and I. Mertig, *Phys. Rev. B* **77**, 224407 (2008).
[20] Youqi Ke, Ke Xia, and Hong Guo, *Phys. Rev. Lett.* **105**, 236801 (2010).
[21] L. O. Chua, *IEEE Trans. Circuit Theory* **18**, 507 (1971).
[22] X. Feng, O. Bengone, M. Alouani, I. Rungger and S. Sanvito, *Phys. Rev. B* **79**, 214432 (2009); X. Feng, O. Bengone, M. Alouani, S. Lebegue, I. Rungger and S. Sanvito, *Phys. Rev. B* **79**, 174414 (2009).
[23] Y. Ikuhara, Y. Sugawara, I. Tanaka and P. Pirouz, *Interface Sci.* **5**, 5 (1997).
[24] A. R. Rocha, V. M. Garcia-Suarez, S. Bailey, C. Lambert, J. Ferrer and S. Sanvito, *Phys. Rev. B* **73**, 085414 (2006).
[25] J. M. Soler, E. Artacho, J. D. Gale, A. Garcia, J. Junquera, P. Ordejon and D. Sanchez-Portal, *J. Phys.: Condens. Matter* **14**, 2745 (2002).
[26] N. Troullier and J. L. Martins, *Phys. Rev. B* **43**, 1993 (1991).
[27] J. P. Perdew and A. Zunger, *Phys. Rev. B* **23**, 5048 (1981).
[28] M. Kurth, P. C. J. Graat and E. J. Mittemeijer, *Thin Solid Films* **500**, 61 (2006).